

Yield correlations and p_T dependence of charm hadrons in Pb + Pb collisions at $\sqrt{s_{NN}} = 2.76$ TeV

Rui-qin Wang,¹ Jun Song,² and Feng-lan Shao^{3,*}

¹*School of Physics, Shandong University, Jinan, Shandong 250100, China*

²*Department of Physics, Jining University, Shandong 273155, China*

³*Department of Physics, Qufu Normal University, Shandong 273165, China*

Recently the ALICE Collaboration has published a few data of charm hadrons in Pb + Pb collisions at the CERN Large Hadron Collider (LHC). We extend the quark combination to the charm sector and point out that the measurement of charm hadron yields can provide important insights into charm quark hadronization mechanism and properties of the hot and dense matter produced in high energy reactions. We propose several types of yield ratios, e.g. D^{*+}/D^0 , D_s^+/D^+ and Λ_c^+/D_s^+ , to measure various properties of low p_T charm quark hadronization. We argue that ratios D_s^+/D^0 and $2D_s^+/(D^0 + D^+)$ as the function of transverse momentum can serve as good probes for the dynamics of charm quark hadronization. We further make predictions for the yields and p_T spectra of identified charm hadrons in central Pb + Pb collisions at $\sqrt{s_{NN}} = 2.76$ TeV.

PACS numbers: 25.75.Ag, 25.75.Dw, 25.75.Gz, 25.75.-q

I. INTRODUCTION

Collisions of heavy nuclei with ultra-relativistic collision energies provide conditions for the creation of a new phase Quark Gluon Plasma (QGP) in the laboratory. Hadrons containing charm quarks are powerful tools to study this high density and strong interacting QGP [1–4]. Measurements on charm hadrons have been executed at the BNL Relativistic Heavy Ion Collider (RHIC) [5, 6] and recently at the CERN Large Hadron Collider (LHC) [7–10]. With the increase of collision energy from RHIC to LHC, the production of charm quarks increases rapidly. At LHC energies, charm quarks produced in QGP stage become comparable to those produced in initial hard rescatterings [11–13]. In addition, re-interactions of charm quarks with partons in QGP also increase with collision energy due to the increasing temperature and energy density of the medium produced in collisions [11–14]. The hadronization of charm quarks is an important topic in charm field since it plays a role of translating these initial or early effects into hadronic observables, and has attracted lots of attentions [15–20]. Quark Combination Mechanism (QCM) is one of the effective phenomenological methods to describe charm quark hadronization. It has shown its success early in studying flavor dependencies of open charm meson and baryon production in elementary hadronic collisions [21–25] and has many applications in heavy ion collisions recently [15–18].

In this paper, we extend the quark combination model in Ref [26, 27] by including charm quarks to study the yield correlations and p_T dependence of charm hadrons in central Pb + Pb collisions at $\sqrt{s_{NN}} = 2.76$ TeV. Hadron yield correlations, measured mainly by the ratios of yields of different hadrons, are one kind of effective probes for the mechanism of hadron production in high energy reactions [27–31]. We study several kinds of two-particle yield ratios such as D^{*+}/D^0 , D_s^+/D^+ and Λ_c^+/D_s^+ as well as four-particle yield correlations, by virtue of which we explore the properties of low p_T charm quark hadronization from different aspects. Furthermore, we study p_T spectra of various charm hadrons based on the explanation of the experimental data of various light and strange hadrons. The p_T dependence of charm meson ratios D_s^+/D^0 and $2D_s^+/(D^0 + D^+)$ are especially selected to probe the dynamics of charm quark hadronization.

The rest of the paper is organized as follows. In Sec. II, we systematically study the yield ratios and multiplicities of charm hadrons in the QCM. In Sec. III, we present the p_T spectra of light, strange and charm hadrons as well as the p_T dependence of charm meson ratios D_s^+/D^0 and $2D_s^+/(D^0 + D^+)$. Sec. IV summaries our work.

II. YIELD CORRELATIONS AND MULTIPLICITIES OF CHARM HADRONS IN THE QCM

In this section, we extend the formulae of hadron yields in Ref [27] to incorporating charm hadrons in the QCM. We discuss several interesting yield ratios of charm hadrons which can reflect various properties in their production and predict the midrapidity hadron yields in central Pb + Pb collisions at $\sqrt{s_{NN}} = 2.76$ TeV.

*Electronic address: shaofl@mail.sdu.edu.cn

A. The formalism of hadron yield

We start with a color-neutral quark-antiquark system with N_{q_i} quarks of flavor q_i and $N_{\bar{q}_i}$ antiquarks of flavor \bar{q}_i . These quarks and antiquarks hadronize via the quark combination. The average numbers for the directly produced mesons M_j and baryons B_j are given by Ref [27],

$$\bar{N}_{M_j}(N_{q_i}, N_{\bar{q}_i}) = \mathcal{P}_{M_j} \bar{N}_M(N_q, N_{\bar{q}}, \sqrt{s_{NN}}) = C_{M_j} \frac{N_{q_1 \bar{q}_2}}{N_{q \bar{q}}} \bar{N}_M(N_q, N_{\bar{q}}, \sqrt{s_{NN}}), \quad (1)$$

$$\bar{N}_{B_j}(N_{q_i}, N_{\bar{q}_i}) = \mathcal{P}_{B_j} \bar{N}_B(N_q, N_{\bar{q}}, \sqrt{s_{NN}}) = N_{iter} C_{B_j} \frac{N_{q_1 q_2 q_3}}{N_{qqq}} \bar{N}_B(N_q, N_{\bar{q}}, \sqrt{s_{NN}}). \quad (2)$$

\bar{N}_M and \bar{N}_B are the average numbers of all mesons and all baryons produced in the system, and they are functions of the total quark number $N_q = \sum_i N_{q_i}$ and antiquark number $N_{\bar{q}} = \sum_i N_{\bar{q}_i}$ due to the flavor-blind property of the strong interaction. Their properties are discussed in detail in Ref [32]. \mathcal{P}_{M_j} is the production weight of a specific meson M_j as a meson is formed. It is determined by the probability of finding a specific $q_1 \bar{q}_2$ pair in all $q \bar{q}$ pairs, $N_{q_1 \bar{q}_2}/N_{q \bar{q}}$, and the flavor branch ratio of M_j in the corresponding flavor-multiplets C_{M_j} , where $N_{q_1 \bar{q}_2} = N_{q_1} N_{\bar{q}_2}$ is the number of all the possible $q_1 \bar{q}_2$ pairs and $N_{q \bar{q}} = N_q N_{\bar{q}}$ the number of all the possible $q \bar{q}$ pairs. Decomposition of \mathcal{P}_{B_j} is similar to \mathcal{P}_{M_j} except an extra N_{iter} which stands for the number of possible iterations of $q_1 q_2 q_3$. It is taken to be 1, 3, and 6 for three identical flavor, two different flavor, and three different flavor cases, respectively. $N_{q_1 q_2 q_3}$ is the number of all the possible $(q_1 q_2 q_3)$'s which satisfies $N_{q_1 q_2 q_3} = N_{q_1} N_{q_2} N_{q_3}$ for $q_1 \neq q_2 \neq q_3$, $N_{q_1 q_2 q_3} = N_{q_1} (N_{q_1} - 1) N_{q_3}$ for $q_1 = q_2 \neq q_3$ and $N_{q_1 q_2 q_3} = N_{q_1} (N_{q_1} - 1) (N_{q_1} - 2)$ for $q_1 = q_2 = q_3$. N_{qqq} is the number of all the possible (qqq) 's, satisfying $N_{qqq} = N_q (N_q - 1) (N_q - 2)$. For flavor branch ratios C_{M_j} and C_{B_j} of charm hadrons, similar to light and strange hadrons, only including $J^P = 0^-$ and 1^- mesons and $J^P = \frac{1}{2}^+$ and $\frac{3}{2}^+$ baryons and using the factors $R_{V/P}$ and/or $R_{O/D}$ to denote the relative production weight of hadrons with the same flavor composition, we have

$$C_{M_j} = \begin{cases} 1/(1 + R_{V/P}) & \text{for } J^P = 0^- \text{ charm mesons} \\ R_{V/P}/(1 + R_{V/P}) & \text{for } J^P = 1^- \text{ charm mesons,} \end{cases} \quad (3)$$

and

$$C_{B_j} = \begin{cases} R_{O/D}/(1 + R_{O/D}) & \text{for } J^P = (1/2)^+ \text{ charm baryons} \\ 1/(1 + R_{O/D}) & \text{for } J^P = (3/2)^+ \text{ charm baryons,} \end{cases} \quad (4)$$

except that $C_{\Lambda_c^+} = C_{\Sigma_c^+} = C_{\Xi_c^0} = C_{\Xi_c'^0} = C_{\Xi_c^+} = C_{\Xi_c'^+} = R_{O/D}/(1 + 2R_{O/D})$, $C_{\Sigma_c^{*+}} = C_{\Xi_c^{*0}} = C_{\Xi_c^{*+}} = 1/(1 + 2R_{O/D})$, and $C_{\Omega_{ccc}^{+++}} = 1$.

For a reaction at a given energy, the average numbers of quarks of different flavors $\langle N_{q_i} \rangle$ and those of antiquarks of different flavors $\langle N_{\bar{q}_i} \rangle$ are fixed while N_{q_i} and $N_{\bar{q}_i}$ follow a certain distribution. In this work, we focus on the midrapidity region at so high LHC energy that the influence of net quarks can be ignored [33]. We suppose a multinomial distribution for both the numbers of u, d, s and c quarks at a given N_q and the numbers of $\bar{u}, \bar{d}, \bar{s}$ and \bar{c} at a given $N_{\bar{q}}$ with the prior probabilities $p_u = p_d = p_{\bar{u}} = p_{\bar{d}} = 1/(2 + \lambda_s + \lambda_c)$, $p_s = p_{\bar{s}} = \lambda_s/(2 + \lambda_s + \lambda_c)$, $p_c = p_{\bar{c}} = \lambda_c/(2 + \lambda_s + \lambda_c)$. Here, we introduce two factors λ_s and λ_c to denote the production suppression of strange quarks and charm quarks, respectively. Averaging over this distribution, Eqs. (1-2) become

$$\bar{N}_{M_j}(N_q, N_{\bar{q}}, \sqrt{s_{NN}}) = C_{M_j} p_{q_1} p_{\bar{q}_2} \bar{N}_M(N_q, N_{\bar{q}}, \sqrt{s_{NN}}), \quad (5)$$

$$\bar{N}_{B_j}(N_q, N_{\bar{q}}, \sqrt{s_{NN}}) = N_{iter} C_{B_j} p_{q_1} p_{q_2} p_{q_3} \bar{N}_B(N_q, N_{\bar{q}}, \sqrt{s_{NN}}). \quad (6)$$

Since yields measured by experiments usually cover only a limited kinematic region, we should also consider the fluctuations of N_q and $N_{\bar{q}}$ in this kinematic region. By averaging over this fluctuation distribution of N_q and $N_{\bar{q}}$ with the fixed $\langle N_q \rangle$ and $\langle N_{\bar{q}} \rangle$, we have

$$\langle N_{M_j} \rangle (\langle N_q \rangle, \langle N_{\bar{q}} \rangle, \sqrt{s_{NN}}) = C_{M_j} p_{q_1} p_{\bar{q}_2} \langle N_M \rangle (\langle N_q \rangle, \langle N_{\bar{q}} \rangle, \sqrt{s_{NN}}), \quad (7)$$

$$\langle N_{B_j} \rangle (\langle N_q \rangle, \langle N_{\bar{q}} \rangle, \sqrt{s_{NN}}) = N_{iter} C_{B_j} p_{q_1} p_{q_2} p_{q_3} \langle N_B \rangle (\langle N_q \rangle, \langle N_{\bar{q}} \rangle, \sqrt{s_{NN}}), \quad (8)$$

where $\langle N_M \rangle$ and $\langle N_B \rangle$ stand for the average total number of the mesons and that of the baryons produced in the combination process.

Finally we incorporate the decay contribution of short lifetime hadrons to obtain

$$\langle N_{h_j}^f \rangle = \langle N_{h_j} \rangle + \sum_{i \neq j} Br(h_i \rightarrow h_j) \langle N_{h_i} \rangle, \quad (9)$$

where the superscript f denotes final hadrons. Decay branch ratio $Br(h_i \rightarrow h_j)$ is given by the Particle Data Group [34].

B. Yield correlations of charm hadrons

From the above discussion, we get that the yields of charm hadrons depend on several physical parameters, e.g., $R_{V/P}$, λ_s and λ_c , etc., which can be seen in Table I for a clear presentation. These parameters, however, can be measured experimentally by the yield ratios between different hadrons. We mainly propose the following four types of particle ratios.

TABLE I: Yields of the directly produced charm hadrons and those including the Strong and ElectroMagnetic (S&EM) decay contributions.

hadrons	directly produced	with S&EM decays
D_s^+	$\frac{1}{1+R_{V/P}} p_c p_{\bar{s}} \langle N_M \rangle$	$p_c p_{\bar{s}} \langle N_M \rangle$
Λ_c^+	$\frac{6R_{O/D}}{1+2R_{O/D}} p_u^2 p_c \langle N_B \rangle$	$12 p_u^2 p_c \langle N_B \rangle$
D^0	$\frac{1}{1+R_{V/P}} p_c p_{\bar{u}} \langle N_M \rangle$	$\frac{1+1.677R_{V/P}}{1+R_{V/P}} p_c p_{\bar{u}} \langle N_M \rangle$
D^+	$\frac{1}{1+R_{V/P}} p_c p_{\bar{u}} \langle N_M \rangle$	$\frac{1+0.323R_{V/P}}{1+R_{V/P}} p_c p_{\bar{u}} \langle N_M \rangle$
D^{*+}	$\frac{R_{V/P}}{1+R_{V/P}} p_c p_{\bar{u}} \langle N_M \rangle$	$\frac{R_{V/P}}{1+R_{V/P}} p_c p_{\bar{u}} \langle N_M \rangle$
D^{*0}	$\frac{R_{V/P}}{1+R_{V/P}} p_c p_{\bar{u}} \langle N_M \rangle$	$\frac{R_{V/P}}{1+R_{V/P}} p_c p_{\bar{u}} \langle N_M \rangle$
J/Ψ	$\frac{R_{V/P}}{1+R_{V/P}} p_c p_{\bar{c}} \langle N_M \rangle$	$\frac{R_{V/P}}{1+R_{V/P}} p_c p_{\bar{c}} \langle N_M \rangle$

First, ratios of D^* to D mesons that can reflect $R_{V/P}$, such as

$$\frac{2\langle N_{D^{*+}}^f \rangle}{\langle N_{D^0}^f \rangle + \langle N_{D^+}^f \rangle} = \frac{R_{V/P}}{1 + R_{V/P}}, \quad \frac{\langle N_{D^{*+}}^f \rangle}{\langle N_{D^0}^f \rangle} = \frac{R_{V/P}}{1 + 1.677R_{V/P}}, \quad \frac{\langle N_{D^{*+}}^f \rangle}{\langle N_{D^+}^f \rangle} = \frac{R_{V/P}}{1 + 0.323R_{V/P}}. \quad (10)$$

By the measurement of these ratios we can quantify $R_{V/P}$, which is helpful for the understanding of the effects of spin interactions during hadronization. Besides, we can also gain the information of $R_{V/P}$ by a yield hierarchy among D mesons. From the results in Table I, we have

$$\langle N_{D^0}^f \rangle : \langle N_{D^{*+}}^f \rangle : \langle N_{D^+}^f \rangle = \frac{1 + 1.677R_{V/P}}{1 + R_{V/P}} : \frac{R_{V/P}}{1 + R_{V/P}} : \frac{1 + 0.323R_{V/P}}{1 + R_{V/P}}, \quad (11)$$

and then we get $\langle N_{D^0}^f \rangle > \langle N_{D^{*+}}^f \rangle > \langle N_{D^+}^f \rangle$ when $R_{V/P} > 1.477$ while $\langle N_{D^0}^f \rangle > \langle N_{D^+}^f \rangle > \langle N_{D^{*+}}^f \rangle$ when $R_{V/P} < 1.477$. Since the mass discrepancy between D^* and D is much smaller than that in light and strange hadrons, one could expect D^* is not much suppressed relative to D and $R_{V/P}$ might approach 3 by counting the spin degree of freedom. We note that $R_{V/P}$ has been observed to approximately equal to 3 in charm sector in pp collisions at LHC [35]. In this case Eqs. (10-11) are easily tested by the experiments.

Second, ratios between D_s and D mesons that can reflect the strangeness suppression factor λ_s , e.g.,

$$\frac{2\langle N_{D_s^+}^f \rangle}{\langle N_{D^0}^f \rangle + \langle N_{D^+}^f \rangle} = \lambda_s, \quad \frac{\langle N_{D_s^+}^f \rangle}{\langle N_{D^0}^f \rangle} = \frac{1 + R_{V/P}}{1 + 1.677R_{V/P}} \lambda_s, \quad \frac{\langle N_{D_s^+}^f \rangle}{\langle N_{D^+}^f \rangle} = \frac{1 + R_{V/P}}{1 + 0.323R_{V/P}} \lambda_s. \quad (12)$$

In the QCM, a charm quark captures a light or a strange antiquark to form a D meson or a D_s meson, so ratios of these D_s to D mesons carry the strangeness information of the production zone of these open charm mesons. By virtue of the strangeness, these ratios can effectively probe the hadronization environment of charm quarks, i.e., inside or outside the QGP. It is known that in relativistic heavy ion collisions the produced bulk quark matter has the saturated strangeness which is about 0.40-0.45, while for the small partonic system such as that created in pp collisions the strangeness is only about 0.3 [35]. Therefore, if these ratios measured by experiments tend to the saturated value, this means charm quarks mainly hadronize in the QGP, otherwise most of them pass through the QGP and hadronize outside.

Third, ratios that reflect the suppression of charm quarks λ_c , e.g.,

$$\frac{\langle N_{J/\psi}^f \rangle}{\langle N_{D^{*+}}^f \rangle} = \frac{\langle N_{J/\psi}^f \rangle}{\langle N_{D^0}^f \rangle} = \lambda_c, \quad \frac{\langle N_{\Lambda_c^+}^f \rangle}{\langle N_p^f \rangle} = \frac{\langle N_{\Lambda_c^+}^f \rangle}{\langle N_n^f \rangle} = 3\lambda_c, \quad (13)$$

where we use $\langle N_p^f \rangle = \langle N_n^f \rangle = 4p_u^3 \langle N_B \rangle$ obtained in our previous work [27]. These ratios provide the direct measurement of the production suppression of charm quarks relative to light quarks.

Fourth, ratios that reflect the baryon-meson competition in the charm sector, e.g.,

$$\frac{\langle N_{\Lambda_c^+}^f \rangle}{\langle N_{D^0}^f \rangle + \langle N_{D^+}^f \rangle} = \frac{6}{2 + \lambda_s + \lambda_c} \frac{\langle N_B \rangle}{\langle N_M \rangle}, \quad \frac{\langle N_{\Lambda_c^+}^f \rangle}{\langle N_{D^+}^f \rangle} = \frac{12}{\lambda_s(2 + \lambda_s + \lambda_c)} \frac{\langle N_B \rangle}{\langle N_M \rangle}. \quad (14)$$

Because of small decay contaminations, these ratios provide a clean measurement of baryon and meson production competition.

In addition, we can build more sophisticated combinations of the average yields of different hadrons such as

$$\frac{\langle N_{D^+}^f \rangle \langle N_{\Xi^-}^f \rangle}{(\langle N_{D^0}^f \rangle + \langle N_{D^+}^f \rangle) \langle N_{\Omega^-}^f \rangle} = \frac{3}{2}, \quad \frac{\langle N_{\Lambda_c^+}^f \rangle \langle N_{D^{*+}}^f \rangle}{\langle N_p^f \rangle \langle N_{J/\psi}^f \rangle} = 3, \quad (15)$$

where we use $\langle N_{\Xi^-}^f \rangle = 3p_u p_s^2 \langle N_B \rangle$ and $\langle N_{\Omega^-}^f \rangle = p_s^3 \langle N_B \rangle$ [27]. These two relations are independent of the above parameters. Therefore, they are characteristics of the QCM and can be used for the first test of the QCM.

C. Predictions for charm hadron yields

Now we turn to the predictions of the midrapidity yields dN/dy of various hadrons in central Pb + Pb collisions at $\sqrt{s_{NN}} = 2.76$ TeV. We first fix the necessary inputs. The rapidity density of all quarks dN_q/dy is fixed to be 1731 by fitting the measured pseudorapidity density of charged particles [36, 37]. The strangeness suppression factor λ_s is taken to be the saturation value 0.41 and then we get the rapidity density of strange quarks $\frac{dN_s}{dy} = \frac{\lambda_s}{2 + \lambda_s + \lambda_c} \frac{dN_q}{dy} \approx \frac{\lambda_s}{2 + \lambda_s} \frac{dN_q}{dy}$. Charm quark number which is related to the suppression factor λ_c by $\frac{dN_c}{dy} = \frac{\lambda_c}{2 + \lambda_s + \lambda_c} \frac{dN_q}{dy}$ is the key input for predictions of charm hadron yields.

The production of charm quarks at LHC mainly comes from two stages of the collision: initial hard-parton scatterings and thermal partonic interactions in the QGP. Here we first give an estimation of charm quark number dN_c/dy from initial hard scatterings by extrapolating pp reaction data at LHC,

$$\frac{dN_c^{PbPb}}{dy} = \frac{1}{R} \frac{dN_{D^0}^{PbPb}}{dy} = \frac{1}{R} < T_{AA} > \frac{d\sigma_{D^0}^{pp}}{dy} = 21 \pm 6. \quad (16)$$

Here $R = 0.54 \pm 0.05$ is the branch ratio of charm quarks into final D^0 mesons measured in e^+e^- reactions [6]. $< T_{AA} > = 26.4 \pm 0.5 \text{ mb}^{-1}$ is the average nuclear overlap function calculated with the Glauber model [38]. The cross section of D^0 is $\frac{d\sigma_{D^0}^{pp}}{dy} = 0.428 \pm 0.115 \text{ mb}$ in pp reactions at $\sqrt{s} = 2.76 \text{ TeV}$ [7].

Subsequent QGP evolution stage can increase the charm quark number but the enhancement is sensitive to the evolution details such as initial temperature, charm quark mass, evolution time, etc, which lead to that the present predictions of charm quark number in literatures have a large uncertainties [11–13]. Here, we consider the largest uncertainty predicted by Ref [11] which is up to 100%, i.e., $\frac{dN_c}{dy} = 21_{-6}^{+27}$, to predict charm hadron yields and their uncertainties. The predicted yields of various charm hadrons as well as light and strange hadrons are shown in Table II, and the data are from Refs [33, 39, 40]. Here, the remaining parameter $R_{V/P}$ is taken to be 3 by the spin counting and $R_{O/D}$ is taken to be 2, the same as in the light and strange sectors. The results for light and strange hadrons are consistent with the available data within the experimental uncertainties.

Note that the current prediction of ϕ mesons might be higher than the future datum. This is because that in this paper we only consider the production of SU(4) hadrons within the quark model. In fact, various multi-quark states and/or exotic states beyond the quark model are also produced in high energy reactions. There are two exotic hadrons, i.e. $f_0(980)$ and $a_0(980)$, that are mostly relevant to the ϕ production abundance. The masses of these two hadrons are close to ϕ and they also probably have the large $s\bar{s}$ content according to the newest PDG [34]. Including these two hadrons in our model will consume $s\bar{s}$ pairs in the system and introduce the competition against the ϕ formation. According to the experimental data in e^+e^- annihilations [34] and our previous study at top SPS [26], we estimate the practical ϕ yield in central Pb + Pb collisions at $\sqrt{s_{NN}} = 2.76 \text{ TeV}$ might be about 14, i.e. only a half of current prediction.

III. p_T DEPENDENCE OF LIGHT, STRANGE AND CHARM HADRONS

p_T spectra of identified hadrons, involving the overall multiplicity as well as the p_T distribution for each of particle species, can provide more explicit insights into quark hadronization mechanisms and detailed information on the hot and dense bulk matter created in relativistic heavy ion collisions. In the QCM, p_T spectra of various light and strange hadrons can be systematically calculated with the given p_T distributions of light and strange quarks. This is one of the main features and advantages of the QCM and has tested against the experimental data at RHIC [29, 30, 41–44]. Here, we test the QCM in explaining p_T

TABLE II: The rapidity densities dN/dy of identified hadrons at $dN_c/dy = 21^{+27}_{-6}$. The data are from Refs [33, 39, 40].

Hadron	Data	Results	Hadron	Data	Results
π^+	733 ± 54	741^{+5}_{-24}	K^+	109 ± 9	110^{+1}_{-4}
K_S^0	110 ± 10	105^{+1}_{-3}	ϕ	—	$29.3^{+0.2}_{-0.9}$
p	34 ± 3	32^{+1}_{-2}	Λ	26 ± 3	25 ± 1
Ξ^-	$3.34 \pm 0.06 \pm 0.24$	$4.01^{+0.04}_{-0.19}$	Ω^-	$0.58 \pm 0.04 \pm 0.09$	$0.55^{+0.01}_{-0.03}$
D^+	—	$3.39^{+4.24}_{-0.96}$	D^0	—	$10.4^{+13.0}_{-3.0}$
D^{*+}	—	$5.16^{+6.46}_{-1.46}$	D_s^+	—	$2.82^{+3.53}_{-0.80}$
J/Ψ	—	$0.15^{+0.65}_{-0.07}$	Λ_c^+	—	$2.82^{+3.43}_{-0.79}$

spectra of identified hadrons at LHC by using a specific Quark Combination Model developed by Shandong Group [26, 45, 46]. For the input distributions of light and strange quarks, we use a two-component parameterized pattern: $d^2N_{q_i}/(p_T dp_T dy) \propto \exp(-\sqrt{p_T^2 + m_{q_i}^2}/T_{q_i}) + R_{q_i}(1 + \frac{p_T}{5\text{GeV}})^{-S_{q_i}}$, the exponential item for thermal quarks at low p_T and power-law item for shower quarks with high p_T . m_{q_i} is the constituent quark mass, and $m_u = m_d = 0.34$ GeV and $m_s = 0.5$ GeV. Parameters ($T_{q_i}, S_{q_i}, R_{q_i}$) for light and strange quarks are extracted by fitting the data of p_T spectra of $\pi^+ + \pi^-$ and Λ , respectively. Their values are (0.31 GeV, 8.0, 0.02) for light quarks and (0.36 GeV, 8.6, 0.04) for strange quarks.

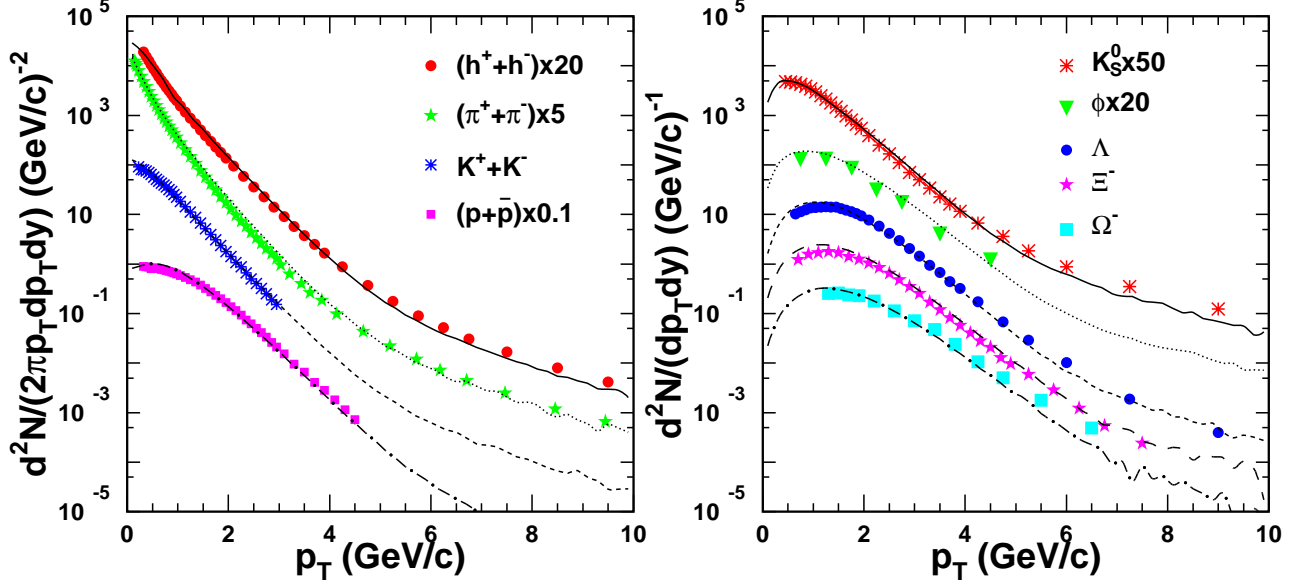


FIG. 1: (Color online) p_T distributions of light and strange hadrons in central Pb + Pb collisions at $\sqrt{s_{NN}} = 2.76$ TeV. The symbols are the experimental data from Refs [33, 38–40, 47, 48]. Charged particles h^\pm are measured in midpseudorapidity, and identified hadrons are in midrapidity. Note that the data of $\pi^+ + \pi^-$ and Λ are used to extract the p_T spectra of light and strange quarks, respectively.

Fig. 1 shows the p_T spectra of h^\pm , π^\pm , K^\pm , K_S^0 , ϕ , p , \bar{p} , Λ , Ξ^- and Ω^- in central Pb + Pb collisions at $\sqrt{s_{NN}} = 2.76$ TeV and the calculated results are consistent with the experimental data [33, 38–40, 47, 48]. This exhibits the validity of the QCM in light and strange sectors at LHC. We see that the exponential domain of meson spectra expands to about 4 GeV/c and that of baryons expands to about 6 GeV/c. Compared with the data at RHIC [49], the exponential domain extends over about 2 GeV/c.

Based on the performance of the QCM in light and strange sectors, we turn to the charm sector. The p_T distribution of charm quarks is the relevant input for the predictions of various charm hadrons. We extract it from the data of D^0 as $d^2N_c/(p_T dp_T dy) \propto (p_T + 0.4\text{GeV})^2(1 + \frac{p_T}{2.2\text{GeV}})^{-8}$. This input is within the theoretical prediction range of charm quark spectrum in Ref [50]. Fig. 2 (a) shows the calculated p_T spectra of D mesons at midrapidity in central Pb + Pb collisions at $\sqrt{s_{NN}} = 2.76$ TeV, from which one can see that within the error uncertainties the results agree with the data from Refs [8, 51].

We argue that the p_T dependence of charm meson ratios D_s^+/D^0 and $2D_s^+/(D^0 + D^+)$ can help explore the dynamical part of charm quark hadronization. These two ratios, as are shown in Eq. (12), are proportional to the strangeness of the production

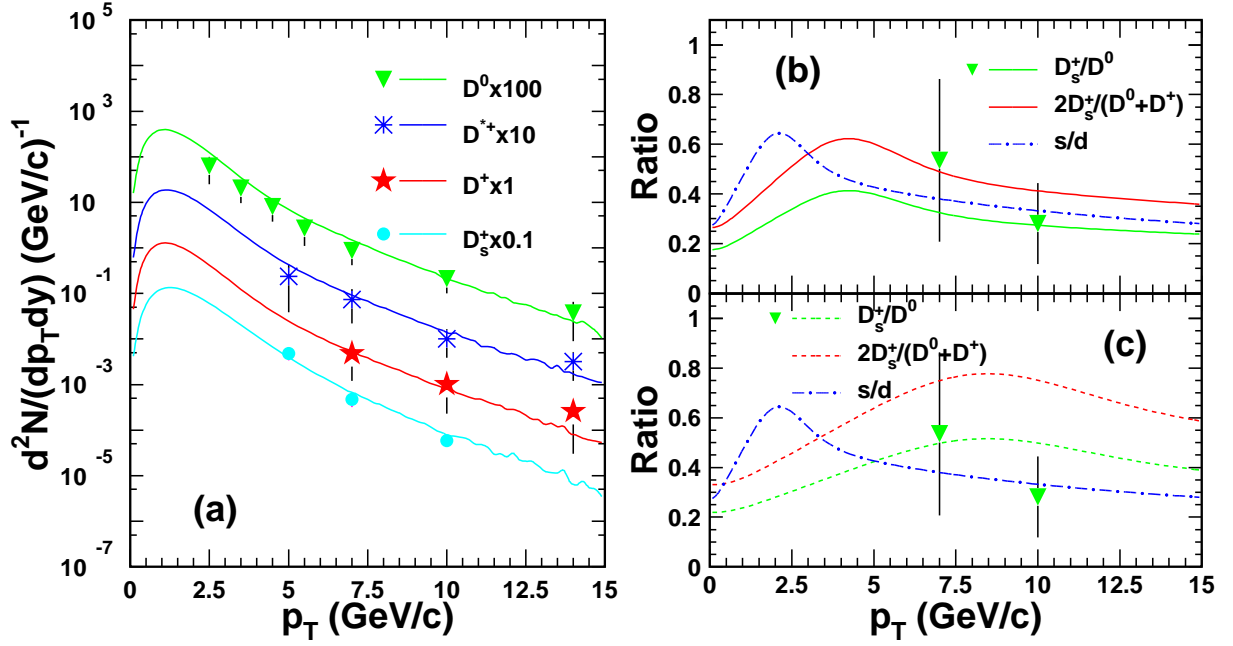


FIG. 2: (Color online) (a) p_T distributions of charm mesons and (b) charm meson ratios in equal p_T combination scenario and (c) charm meson ratios in equal velocity combination scenario at midrapidity in central Pb + Pb collisions at $\sqrt{s_{NN}} = 2.76$ TeV. The filled symbols are the experimental data from Refs [8, 51]. Note that the data of D^0 are used to extract the p_T spectra of charm quarks.

regions of charm mesons. The dot-dashed lines in Fig. 2 (b) and (c) show the p_T dependence of the strangeness, i.e., the ratio of the previously extracted strange quark p_T spectrum to down quark p_T spectrum. It rises rapidly at low p_T and reaches the peak at $p_T \approx 2$ GeV and then it decreases to a stable small value. D_s^+/D^0 and $2D_s^+/(D^0 + D^+)$ as the function of p_T should follow similar sharps by stretching out the p_T axis, but the peak position of the ratios will reflect the detailed combination dynamics of charm hadron formation. The solid lines and dashed lines in panel (b) and (c), respectively, show our predictions of these two ratios in two different combination dynamics, i.e. equal p_T or equal velocity combination, which can not be effectively discriminated in the experimental data of single particle spectra discussed above. Panel (b) shows the results of a charm quark capturing an antiquark with an almost equal p_T to form a meson. The resulting D_s^+/D^0 and $2D_s^+/(D^0 + D^+)$ reach the peak at $p_T \approx 4$ GeV, and decrease to the low values at high p_T . Panel (c) represents the results in case of a charm quark capturing an antiquark with an almost equal velocity to form a meson. In this case, the p_T of charm quark is about triple of that of the antiquark in forming a D meson due to their triple difference in mass. The resulting D_s^+/D^0 and $2D_s^+/(D^0 + D^+)$ will arrive at the peak at $p_T \approx 8$ GeV, which are quite different from those in panel (b). The future experimental data at LHC can check these two different combination scenarios and provide deep insights into the hadronization dynamics of charm quarks in ultra-relativistic heavy ion collisions.

IV. SUMMARY

We have studied in the QCM the yield correlations and p_T spectra of charm hadrons in central Pb + Pb collisions at $\sqrt{s_{NN}} = 2.76$ TeV. Yields of various charm hadrons are found to have a series of interesting correlations. Several types of yield ratios were proposed to quantify these correlations and to measure the properties of charm quark hadronization from different aspects. In addition, we used the p_T spectra of light and strange quarks extracted from the data of $\pi^+ + \pi^-$ and Λ , only two inputs, to systematically explain the midrapidity data of p_T spectra for h^\pm , K^\pm , K_s^0 , ϕ , p , \bar{p} , Ξ^- and Ω^- . We further calculated the p_T spectra of open charm mesons and found that the results agree with the available experimental data. Ratios D_s^+/D^0 and $2D_s^+/(D^0 + D^+)$ as the function of p_T are identified as good probes for the hadronization dynamics of charm quarks, and we made predictions in two different combination scenarios for the comparison with the future experimental data.

Acknowledgements

The authors thank Z. T. Liang, Q. B. Xie, Q. Wang, H. J. Xu, W. Wang and the members of the particle theory group of Shandong University for helpful discussions. This work is supported in part by the National Natural Science Foundation of

China under grant 11175104, 11305076, 11247202, and by the Natural Science Foundation of Shandong Province, China under grant ZR2011AM006, ZR2012AM001.

-
- [1] T. Matsui and H. Satz, Phys. Lett. B **178**, 416 (1986).
 - [2] H. van Hees, V. Greco, and R. Rapp, Phys. Rev. C **73**, 034913 (2006).
 - [3] Á. Mócsy and P. Petreczky, Phys. Rev. Lett. **99**, 211602 (2007).
 - [4] M. He, R. J. Fries, and R. Rapp, Phys. Rev. Lett. **110**, 112301 (2013).
 - [5] S. S. Adler *et al.* (PHENIX Collaboration), Phys. Rev. Lett. **94**, 082301 (2005).
 - [6] J. Adams *et al.* (STAR Collaboration), Phys. Rev. Lett. **94**, 062301 (2005).
 - [7] B. Abelev *et al.* (ALICE Collaboration), JHEP **1207**, 191 (2012).
 - [8] B. Abelev *et al.* (ALICE Collaboration), JHEP **09**, 112 (2012).
 - [9] G. Luparello (for the ALICE Collaboration), J. Phys. Conf. Ser. **446**, 012039 (2013).
 - [10] H. Yang (for the ALICE Collaboration), Nucl. Phys. A **904-905**, 673c-676c, (2013).
 - [11] P. Lévai and R. Vogt, Phys. Rev. C **56**, 2707 (1997).
 - [12] J. Uphoff, O. Fochler, Z. Xu, and C. Greiner, Phys. Rev. C **82**, 044906 (2010).
 - [13] B. W. Zhang, C. M. Ko, and W. Liu, Phys. Rev. C **77**, 024901 (2008).
 - [14] K. Zhou, N. Xu, and P. F. Zhuang, arXiv:1309.7520v1 [nucl-th].
 - [15] V. Greco, C. M. Ko, and R. Rapp, Phys. Lett. B **595**, 202 (2004).
 - [16] T. Yao, W. Zhou, and Q. B. Xie, Phys. Rev. C **78**, 064911 (2008).
 - [17] Y. Oh, C. M. Ko, S. H. Lee, and S. Yasui, Phys. Rev. C **79**, 044905 (2009).
 - [18] Y. P. Liu, C. Greiner, and A. Kostyuk, Phys. Rev. C **87**, 014910 (2013).
 - [19] M. He, R. J. Fries, and R. Rapp, Phys. Rev. C **86**, 014903 (2012).
 - [20] H. J. Xu, X. Dong, L. J. Ruan, Q. Wang, Z. B. Xu, and Y. F. Zhang, arXiv:1305.7302v1 [nucl-th].
 - [21] R. C. Hwa, Phys. Rev. D **51**, 85 (1995).
 - [22] J. C. Anjos, J. Magnin, and G. Herrera, Phys. Lett. B **523**, 29 (2001).
 - [23] E. Braaten, Y. Jia, and T. Mehen, Phys. Rev. Lett. **89**, 122002 (2002).
 - [24] R. Rapp and E. V. Shuryak, Phys. Rev. D **67**, 074036 (2003).
 - [25] T. Mehen, J. Phys. G **30**, S295 (2004).
 - [26] C. E. Shao, J. Song, F. L. Shao, and Q. B. Xie, Phys. Rev. C **80**, 014909 (2009).
 - [27] R. Q. Wang, F. L. Shao, J. Song, Q. B. Xie, and Z. T. Liang, Phys. Rev. C **86**, 054906 (2012).
 - [28] P. Braun-Munzinger, J. Stachel, J. P. Wessels, and N. Xu, Phys. Lett. B **344**, 43(1995).
 - [29] R. C. Hwa and C. B. Yang, Phys. Rev. C **70**, 024905 (2004).
 - [30] V. Greco, C. M. Ko, and I. Vitev, Phys. Rev. C **71**, 041901 (2005).
 - [31] J. Zimányi, T. S. Biró, T. Csörgő, and P. Lévai, Phys. Lett. B **472**, 243 (2000).
 - [32] J. Song and F. L. Shao, Phys. Rev. C **88**, 027901 (2013).
 - [33] B. Abelev *et al.* (ALICE Collaboration), Phys. Rev. Lett. **109**, 252301 (2012).
 - [34] J. Beringer *et al.* (Particle Data Group), Phys. Rev. D **86**, 010001 (2012).
 - [35] B. Abelev *et al.* (ALICE Collaboration), Phys. Lett. B **718**, 279 (2012).
 - [36] K. Aamodt *et al.* (ALICE Collaboration), Phys. Rev. Lett. **106**, 032301 (2011).
 - [37] T. Yao, The Study of Universality for Quark Combination Mechanism in QGP Hadronization Process, Ph.D. thesis, Shandong University, 2009.
 - [38] K. Aamodt *et al.* (ALICE Collaboration), Phys. Lett. B **696**, 30 (2011).
 - [39] B. Abelev *et al.* (ALICE Collaboration), arXiv:1307.5530v1 [nucl-ex].
 - [40] B. Abelev *et al.* (ALICE Collaboration), arXiv:1307.5543v1 [nucl-ex].
 - [41] R. C. Hwa and C. B. Yang, Phys. Rev. C **75**, 054904 (2007).
 - [42] L. W. Chen and C. M. Ko, Phys. Rev. C **73**, 044903 (2006).
 - [43] Y. F. Wang, F. L. Shao, J. Song, D. M. Wei, and Q. B. Xie, Chin. Phys. C **32**, 976-983 (2008).
 - [44] K. Zhang, J. Song and F. L. Shao, Phys. Rev. C **86**, 014906 (2012).
 - [45] Q. B. Xie and X. M. Liu, Phys. Rev. D **38**, 2169 (1988).
 - [46] F. L. Shao, Q. B. Xie, and Q. Wang, Phys. Rev. C **71**, 044903 (2005).
 - [47] P. Christiansen (for the ALICE Collaboration), arXiv:1208.5368v1 [nucl-ex].
 - [48] A. G. Knospe (for the ALICE Collaboration), J. Phys. Conf. Ser. **420**, 012018 (2013).
 - [49] B. I. Abelev *et al.* (STAR Collaboration), Phys. Rev. Lett. **97**, 152301 (2006).
 - [50] H. van Hees and R. Rapp, Phys. Rev. C **71**, 034907 (2005).
 - [51] G. M. Innocenti (for the ALICE Collaboration), Nucl. Phys. A **904-905**, 433c-436c, (2013).